



Published in final edited form as:

*Nanomedicine (Lond)*. 2009 June ; 4(4): 421–429. doi:10.2217/nnm.09.24.

## Hyaluronan- and heparin-reduced silver nanoparticles with antimicrobial properties

Melissa M Kemp<sup>1</sup>, Ashavani Kumar<sup>4</sup>, Dylan Clement<sup>5</sup>, Pulickel Ajayan<sup>4</sup>, Shaker Mousa<sup>5</sup>, and Robert J Linhardt<sup>1,2,3</sup>

<sup>1</sup>Department of Biology, Rensselaer Polytechnic Institute, Troy, NY 12180, USA

<sup>2</sup>Department of Chemistry & Chemical Biology, Rensselaer Polytechnic Institute, NY, USA

<sup>3</sup>Department of Chemical & Biological Engineering, Rensselaer Polytechnic Institute, NY, USA Tel.: +1 518 276 3404; E-mail: linhar@rpi.edu

<sup>4</sup>Department of Mechanical Engineering & Materials Science, Rice University, Houston, TX, USA

<sup>5</sup>The Pharmaceutical Research Institute, Albany College of Pharmacy, Albany, NY, USA

### Abstract

**Aims**—Silver nanoparticles exhibit unique antibacterial properties that make these ideal candidates for biological and medical applications. We utilized a clean method involving a single synthetic step to prepare silver nanoparticles that exhibit antimicrobial activity.

**Materials & methods**—These nanoparticles were prepared by reducing silver nitrate with diaminopyridinylated heparin (DAPHP) and hyaluronan (HA) polysaccharides and tested for their efficacy in inhibiting microbial growth.

**Results & discussion**—The resulting silver nanoparticles exhibit potent antimicrobial activity against *Staphylococcus aureus* and modest activity against *Escherichia coli*. Silver–HA showed greater antimicrobial activity than silver–DAPHP, while silver–glucose nanoparticles exhibited very weak antimicrobial activity. Neither HA nor DAPHP showed activity against *S. aureus* or *E. coli*.

**Conclusion**—These results suggest that DAPHP and HA silver nanoparticles have potential in antimicrobial therapeutic applications.

### Keywords

antimicrobial; *Escherichia coli*; silver heparin nanoparticles; silver hyaluronan nanoparticles; silver nanoparticles; *Staphylococcus aureus*

---

Metal nanoparticles (NPs) have recognized importance in chemistry, physics and biology because of their unique optical, electrical and photothermal properties [1–6]. Such metallic NPs have potential applications in laboratory settings such as analytical chemistry and have been used as probes in mass spectroscopy [7], as well as in colorimetric detection for proteins and DNA [8]. Metal NPs have also been used for therapeutic applications and drug delivery [9,10]. For many years, silver (Ag) has been known to exhibit antibacterial properties and this characteristic has been exploited in a wide variety of applications, such as catheters [11], prostheses [12], textiles [13,14] and water treatment [15]. The mechanisms for this antimicrobial property is only partially understood. It has been hypothesized that positively charged Ag ions (Ag<sup>+</sup>) are able to interact with the negatively charged bacterial cell wall, inhibiting membrane

permeability [16], and inactivating necessary enzymes by interacting with the thiol groups of the proteins [17,18], leading to cell death.

Silver NPs (AgNPs) also have the same intrinsic antimicrobial properties. The molecular mechanism for this antimicrobial activity has been hypothesized to result from the oxidation of metallic Ag ( $\text{Ag}^0$ ) to  $\text{Ag}^+$  on exposure to aqueous solutions containing oxidizing agents [19]. AgNPs are of interest because they offer slow, controlled release of  $\text{Ag}^+$ . The surface of AgNPs is exposed to aqueous oxidants forming  $\text{Ag}^+$ , which can then deactivate the proteins necessary for bacteria, viruses and fungi to survive. The slow release of  $\text{Ag}^+$  ions from AgNPs avoids the excess delivery of  $\text{Ag}^+$  that can result from the use of Ag salts. Moreover, AgNPs are less susceptible to deactivation by the chloride ions in physiological media than Ag salts [19]. NPs have a high ratio of surface area per unit mass, resulting in greater antimicrobial activity and more controlled release of  $\text{Ag}^+$  ions [20–22].

Various methods have been reported over the last two decades for the synthesis of AgNPs. These involve the reduction of metal salts with a chemical reducing agent, such as sodium citrate, sodium borohydride or other organic compounds [23–26] that introduce contaminants, which are often toxic. One area that is being actively explored relies on carbohydrates as the reducing agents. Raveendran *et al.* used glucose as the reducing agent and starch as a capping agent to prepare starch AgNPs [27]. Huang *et al.* used chitosan and heparin (HP) as reducing and stabilizing agents for the synthesis of gold NPs and AgNPs, respectively [28]. Previous studies evaluated the synthesis of these AgNPs using carbohydrates, but few evaluate their antimicrobial activities, especially with large carbohydrates such as glycosaminoglycans (GAGs).

Glycosaminoglycans are negatively charged polysaccharides composed of repeating disaccharides units. These include HP, heparan sulfate, chondroitin sulfate, hyaluronan (HA), dermatan sulfate and keratan sulfate, each having important and diverse biological functions. Some GAGs, such as HP, are often found attached through their reducing ends to core proteins. These form larger macromolecules, called proteoglycans. Proteoglycans have diverse biological functions depending on both the core protein and the type and number of GAG chains that are attached. Pharmaceutical HP is released from its core protein and is used as an anticoagulant. It also has activities in promoting wound healing and angiogenesis, as well as inhibiting tumor metastasis and inflammation [29]. HA is biosynthesized free of a core protein and serves as a lubricant and shock absorber in the extracellular matrix; it is also involved in the mediation of cellular proliferation and migration [30]. HA has also been medicinally used for treating joint disease and promoting wound healing [31]. These molecules are biologically friendly and have a number of therapeutic applications. However, GAGs are also sugars and can support microbial growth when used in wound healing applications. Currently, GAGs have been used for medical applications such as wound healing in combination with external antimicrobial agents, such as iodine. In this study, we examine GAG-based bioconjugates designed to exhibit their natural pharmacology along with antimicrobial activity, inhibiting the growth of bacteria.

Previously, we demonstrated the synthesis of gold NPs and AgNPs, using HP derivatized with a diaminopyridinyl (DAP) group and HA, which were stable and showed anticoagulant and anti-inflammatory properties [32]. The current study examines the potential pharmacological and antimicrobial activity of AgNPs synthesized using GAGs. This clean synthetic method relies on HP and HA as reducing and stabilizing agents, eliminating the impurities that conventional reduction methods introduce, and affording stable NPs with antimicrobial activity. These NPs might be useful for treatment of burns or in wound healing by promoting cellular proliferation (re-epithelialization) while inhibiting inflammation and microbial infection.

## Materials & methods

### Materials

Silver nitrate, HA sodium salt from *Streptococcus equi*, sodium chloride, calcium chloride and heparinase I (E.C. 4.2.2.7) from *Flavobacterium heparinum* and Dowex-1 strongly basic anion-exchange resin were purchased from Sigma Chemicals (St Louis, MO, USA) and used as received. HP sodium from porcine intestinal mucosa was purchased from Celsus Laboratories (Cincinnati, OH, USA), and *Escherichia coli* (25922) and *Staphylococcus aureus* (27660) were obtained from the American Type Culture Collection. Other common reagents were ordered from Sigma Chemicals.

### Synthesis of AgNPs capped with DAPHP

The method of synthesizing 2,6-diaminopyridinyl HP (DAPHP) is described elsewhere [33]. Briefly, HP (100 mg, 8.3  $\mu$ M) was dissolved in 1 ml of formamide by heating at 50°C. The 2,6-diaminopyridine (100 mg, 920  $\mu$ M) was then added to the mixture and the reaction was maintained at 50°C for 6 h. An aqueous solution of sodium cyanoborohydride (9.5 mg, 150  $\mu$ M) was added and the temperature was maintained at 50°C for an additional 24 h. A total of 10 ml of water was added to dilute the reaction mixture and dialyzed against 2 l of water using a 1000 molecular weight cut-off dialysis membrane for 48 h. The sample was then recovered, lyophilized and purified by methanol precipitation and strong anion exchange chromatography on Dowex-1 resin.

The AgNPs were formed using DAPHP and AgNO<sub>3</sub>. Typically, an aqueous solution of AgNO<sub>3</sub> (0.1 mM) was heated until boiling. DAPHP (0.5 mM aqueous solution) was then added dropwise to AgNO<sub>3</sub> and the solution was boiled for 20 min. The DAPHP reduction of AgNO<sub>3</sub> to AgNPs could be monitored by observing the change of color from light yellow to dark yellow. The mixture could be purified by recovering the Ag–DAPHP NPs by centrifugation at 16,000  $\times$  g for 20 min and washing with water three times. However, for the antimicrobial assay the nanocomposites were used without further purification, since a better comparison can be made with the other AgNPs that were reduced with HA and glucose. The stability of the particles was tested using various concentrations of NaCl. Different amounts of NaCl were added to a solution of AgNPs, after which the UV-visible (UV-Vis) spectrum was taken. The particles were sterilized by autoclaving, using conditions under which HP and HA are known to be stable (120°C for 20 min).

### Synthesis of AgNPs with HA

Typically, an aqueous solution of 0.1 mM HA was gradually heated to dissolve the HA. Approximately 200  $\mu$ g of AgNO<sub>3</sub> in 1 ml of water was added dropwise to the HA solution for a final concentration of 0.1 mM. The solution was gradually heated and incubated in a 70°C water bath overnight. The formation of AgNPs was observed by monitoring the change of color from light yellow to dark yellow. The stability of the particles was tested using various concentrations of NaCl. Different amounts of NaCl were added to a solution of AgNPs, after which the UV-Vis spectrum was taken. Particles were autoclaved for sterilization in the same manner as the Ag–DAPHP NPs.

### Synthesis of AgNPs with glucose

An aqueous solution of glucose (55 mM) was heated and stirred until boiling. An aqueous solution of AgNO<sub>3</sub> was added dropwise to the glucose solution for a final concentration of 0.1 mM. The formation of particles was monitored by the change of color from light yellow to dark yellow. Particles were sterilized by filtration through a 0.22  $\mu$ m syringe filter.

## Characterization of AgNPs

Various spectroscopic techniques including UV-Vis, field emission scanning electron microscopy and transmission-electron microscopy (TEM) were used to characterize the nanocomposites. UV-Vis spectroscopic measurements of the particles relied on a LAMDA 950 UV/Vis/NIR Spectrometer (Perkin Elmer, USA) operated with a resolution of 2 nm. The morphology of the nanostructures was characterized by scanning-electron microscopy in a JEOL (Peabody, MA, USA) 6330 F field emission scanning electron microscope operated at 5 kV. TEM was used to determine the size distribution of the particles on a Philips (FEI, Hillsboro, OR, USA) CM12 TEM.

## Activated partial thromboplastin time assay

The activated partial thromboplastin time (aPTT) assay is a standard coagulation assay that determines the clotting time of activated, recalcified plasma [34]. Ag-DAPHP, DAPHP and Ag-glucose samples were added, respectively, to 100  $\mu$ l of automated aPTT reagent to cups and warmed at 37°C for 1 min; 100  $\mu$ l of citrated plasma was added and warmed 5 min at 37°C. A 100  $\mu$ l aliquot of pre-warmed CaCl<sub>2</sub> (0.025 M) was added to recalcify the citrated plasma, the fibrometer was immediately started and the clotting time was measured. The fibrometer was stopped after 10 min, if it did not stop automatically. Each concentration was performed in triplicate.

## Minimum inhibition concentration assay

The assay is a modification of the standard micro-broth dilution assay recommended by the National Committee for Clinical Laboratory Standards (NCCLS, USA), which has been developed for determining *in vitro* antimicrobial activities of cationic agents [35,36]. The modifications were made to minimize loss of the antimicrobial agent due to adsorption onto glass or plastic surfaces and by precipitation at high concentrations. The protocol carried out is briefly described: bacteria were grown by taking 10  $\mu$ l of frozen bacteria strains (*E. coli* and *S. aureus*) into 3 ml of cation-adjusted (340 mM NaCl) Mueller-Hinton Medium II, and incubating overnight at 37°C on a shaker. Growth was monitored by a spectrophotometer at OD<sub>600</sub> by diluting 1:10 into Mueller-Hinton Medium II; the blank was Mueller-Hinton II medium. Each strain was diluted to obtain a working solution of OD<sub>600</sub> = 0.001 (or  $\sim 10^6$  cfu/ml). A total of 11 1:2 serial dilutions of the Ag samples in sterile water were prepared and 10  $\mu$ l of each of the diluted compounds were added to a 96-well round-bottom polypropylene plate. Diluted bacterial strains (90  $\mu$ l) were added to the respective wells in duplicate and incubated for 18 h at 37°C. The minimum inhibitory concentration was measured by observing bacteria growth defined by NCCLS as a 2 mm or greater button or where turbidity is clearly observed.

## Results & discussion

### Synthesis & characterization of Ag-HA & Ag-DAPHP

Heparin derivatized with a DAP group at the reducing end was synthesized through reductive amination. Residual underivatized HP present in the DAPHP preparation has the ability to reduce the Ag salts, while the amino group of the DAP moiety provides a strong interaction with the AgNPs. The reducing end of HA chains are also able to reduce AgNO<sub>3</sub> forming AgNPs. These GAGs are very polydisperse with estimated molecular weights for HA and DAPHP of approximately 100 and 12 KDa, respectively. These molecular weights were used to determine the concentration of GAGs for synthesis and for *in vitro* experiments. Because of the large size and polydispersity of these GAGs, end-group analysis was impracticable. The concentration of GAGs used was an approximate 1:1 ratio of the amount of AgNO<sub>3</sub> that was used, corresponding to approximately 1  $\mu$ M of GAG for approximately 1  $\mu$ M of AgNO<sub>3</sub>. The

nanocomposites prepared were analyzed by UV-Vis spectroscopy. The UV-Vis spectra recorded on AgNP solutions synthesized using HA, DAPHP and glucose are shown in Figure 1. A strong resonance at approximately 400–450 nm is observed for Ag–DAPHP, Ag–HA and Ag–glucose NPs in solution, due to the excitation of surface plasmon vibrations. The pH of the corresponding solutions was measured and ranged from 4 to 6, being buffered by the carboxyl groups in these polysaccharides. While this is below physiological pH, no external buffer was added, as this would only confound our analysis. It should be noted that at physiologic pH these NPs would have added negative charge, resulting from the full ionization of the polysaccharide carboxyl groups, and thus a further reduction in their propensity to aggregate.

The instability of NPs, particularly in the presence of electrolytes, is a major problem in colloidal chemistry. Electrolyte-induced precipitation of NPs from the aqueous phase is commonly observed. Their stability was tested at different NaCl concentrations to determine if they would aggregate at physiological salt conditions, which is approximately 150 mM. The stability of these NPs was studied for both Ag–HA and Ag–DAPHP in the presence of increasing NaCl concentrations (Figure 2A & B). Unpurified Ag–DAPHP was stable up to 1 M NaCl concentration, as well as Ag–HA up to 1 M NaCl. However, for purified Ag–DAPHP, the limit of NaCl concentration was approximately 150 mM (data not shown). The high stability of Ag–HA at physiologic salt concentrations may be due to the thick gel that forms, hindering the coalescence of AgNPs, thus preventing their aggregation. Ag–DAPHP was also quite stable at high salt concentrations (Figure 2A), but when purified, the maximum NaCl concentration that the particles could withstand was approximately 150 mM. The decreased stability of purified samples is probably related to the decreased amount of weakly bound HP present in the sample. The presence of HP results in an electrostatic repulsion between the NPs. Salt disrupts this repulsion and a decreased level of HP on NPs requires less NaCl to neutralize the charges and enhance NP aggregation.

2,6-diaminopyridinyl heparin and HA synthesized AgNPs were further characterized using TEM to visualize morphology and size of the particles. A drop-coated film of aqueous solution of NPs was formed on carbon-coated copper grid by solvent evaporation and analyzed by TEM. TEM images of the Ag–DAPHP showed that these particles are monodisperse with the majority of the particles ranging from  $11 \pm 3$  nm (Figure 3A & B). There were a small percentage of particles that were larger. TEM images of Ag–HA films formed on a copper grid and the particle-size distribution are shown in Figure 4A & B. The Ag–HA was more polydisperse than the Ag–DAPHP, with a larger size distribution and more diverse morphologies. The particles looked to be embedded within the surrounding HA matrix (Figure 4B). The surface morphology of Ag–HA was examined using scanning-electron microscopy (Figure 5). The Ag–HA particles appear to have a rough surface morphology, with many indentations and shapes. The narrow size distribution observed for Ag–DAPHP can be explained by the interaction between the amine on the DAP moiety and the AgNPs that controls the size and morphology of the NPs. The interaction between HA and the AgNPs is weaker than DAPHP with the AgNPs, resulting in larger and more disperse particle formation. The HA in the AgNP, however, affords a more viscous solution, leading to improved stability. The high stability of Ag–DAPHP and Ag–HA was also demonstrated by similarity of the UV-Vis peaks before and after autoclaving. The increase in the peak intensity for both Ag–DAPHP and Ag–HA after autoclaving can be explained by the heat and pressure driving to completion the reduction of AgNO<sub>3</sub> by HA and DAPHP (Figures 3C & 4C).

### Antimicrobial activity of Ag–HA & Ag–DAPHP

The sterilized Ag–DAPHP and Ag–HA particles were investigated to see if they possessed any antimicrobial activity against *S. aureus* and *E. coli*. The synthesized Ag–DAPHP and Ag–HA

particles were sterilized by autoclaving and the particles were confirmed to still be stable by UV-Vis indicated by similar peak profiles (Figures 3C & 4C). Our studies showed that AgNPs exhibited antimicrobial efficacy against both *S. aureus* and *E. coli*, with greater efficacy against *S. aureus* (Table 1). Ag-HA showed better antimicrobial activity than Ag-DAPHP, with relatively greater efficacy against *S. aureus* than against *E. coli*. Ag-glucose exhibited weaker antimicrobial activity, 0–10% inhibition at 0.1  $\mu\text{M}$  (Table 1). By contrast, neither HA nor DAPHP showed activity against *S. aureus* or *E. coli* at concentrations up to 1.0  $\mu\text{M}$  (Table 1). The higher activity of Ag-HA, and to a lesser extent Ag-DAPHP, can be explained by the smaller particle size, which leads to a greater surface area, and thus greater antimicrobial effects [20,21]. The lack of antimicrobial activities of HA or DAPHP at concentrations up to 1.0  $\mu\text{M}$  demonstrate that the antimicrobial activity is mainly due to the Ag in the nanocomposites and its potential enhancement with HA or DAPHP. Ag-glucose exhibited only weak antimicrobial activity, possibly due to the larger size of the Ag-glucose NPs. Various studies have showed that toxicity to bacteria is dependent on size of the AgNPs [20,21].

Finally, the heparinized nanocomposites were tested to confirm that they retained the pharmacological activity associated with the GAG itself. The aPTT anticoagulation assay measures the inhibition of the blood coagulation cascade [34]. DAPHP completely prevented coagulation at 3  $\mu\text{g/ml}$ . Ag-DAPHP showed similar anticoagulant activity when 14.5  $\mu\text{g/ml}$  of DAPHP was attached to the AgNPs (Figure 6). Ag-glucose showed no significant anticoagulant activity at comparable AgNP concentrations.

## Conclusion

The main finding in the present study is that Ag-HA and Ag-DAPHP exhibit potent antimicrobial activity. In addition, the aPTT assay clearly confirmed that Ag-DAPHP maintained its pharmacological activity as an anticoagulant. These Ag-HA and Ag-DAPHP particles were stable in aqueous solution over several months when stored at room temperature, showing no signs of aggregation. They also exhibit enhanced stability at physiologic concentrations of NaCl.

The current study demonstrates that AgNP composites can be synthesized and stabilized with both DAPHP and HA. The nanocomposites are much more stable at physiological salt concentrations than naked metallic NPs and have effective antimicrobial activity towards *S. aureus* and *E. coli*. They might potentially be very effective at treating wounds and burns by promoting cellular growth and migration, relieving pain due to the GAGs and preventing microbial contamination due to the presence of AgNPs. These nanocomposites may be useful in a wide variety of biological and biomedical applications that take advantage of the biological activities of HP and HA, as well as the unique physical attributes of Ag-core NPs.

## Future perspective

Important issues remain to be investigated in this work, including the potential for these nanocomposites to be used in medicinal applications, such as wound healing and burn treatment. Moreover, while the interaction of proteins, present in biological fluids, will need to be assessed, we anticipate good biocompatibility as animal cells are covered with similar anionic polysaccharides. GAG chains often elicit different biological responses depending on their size and structure. By using different sized GAGs, or GAGs with different structures, AgNPs might show a completely different biological effect when being used to treat wounds. Therefore, new nanocomposites would need to be evaluated for their cellular compatibility and inflammatory effects, as well as in an *in vivo* model to determine their efficacy in promoting healing and preventing microbial growth.

### Executive summary

Silver nanoparticles (AgNPs) reduced with hyaluronan (HA) and diaminopyridinylated heparin (DAPHP) were highly stable in high NaCl concentrations and during autoclaving for sterilization.

Ag–HA and Ag–DAPHP exhibited unique physical characteristics due to the binding of the glycosaminoglycans onto the AgNPs, which can control the shape and size. Ag–DAPHP was more uniform in shape and size, while Ag–HA appeared rough and irregular on the surface.

Ag–HA and Ag–DAPHP exhibited antimicrobial activity against *Staphylococcus aureus* and *Escherichia coli*. Ag–HA showed stronger antimicrobial activity compared with Ag–DAPHP, possibly due to the indentations and rough surfaces allowing more surface area to be exposed to the environment.

Ag–DAPHP still retained its pharmacological anticoagulant activity, which was tested using an activated partial thromboplastin time assay.

The combination of AgNPs and HA or DAPHP affords active antimicrobial material that can promote wound healing and prevent bacterial contamination.

### Acknowledgments

This research was supported by the NIH (HL62244). The authors have no other relevant affiliations or financial involvement with any organization or entity with a financial interest in or financial conflict with the subject matter or materials discussed in the manuscript apart from those disclosed.

No writing assistance was utilized in the production of this manuscript.

### Bibliography

1. Cognet L, Tardin C, Boyer D, Choquet D, Tamarat P, Lounis B. Single metallic nanoparticle imaging for protein detection in cells. *Proc. Natl Acad. Sci. USA* 2003;100:11350–11355. [PubMed: 13679586]
2. Hirsch LR, Stafford RJ, Bankson JA, et al. Nanoshell-mediated near-infrared thermal therapy of tumors under magnetic resonance guidance. *Proc. Natl Acad. Sci. USA* 2003;100:13549–13554. [PubMed: 14597719]
3. Huang X, El-Sayed IH, Qian W, El-Sayed MA. Cancer cell imaging and photothermal therapy in the near-infrared region by using gold nanorods. *J. Am. Chem. Soc* 2006;128:2115–2120. [PubMed: 16464114]
4. Li J, Wang X, Wang C, et al. The enhancement effect of gold nanoparticles in drug delivery and as biomarkers of drug-resistant cancer cells. *ChemMedChem* 2007;2:374–378. [PubMed: 17206735]
5. O'Neal DP, Hirsch LR, Halas NJ, Payne JD, West JL. Photo-thermal tumor ablation in mice using near infrared-absorbing nanoparticles. *Cancer Lett* 2004;209:171–176. [PubMed: 15159019]
6. Skirtach AG, Dejugnat C, Braun D, et al. The role of metal nanoparticles in remote release of encapsulated materials. *Nano Lett* 2005;5:1371–1377. [PubMed: 16178241]
7. Shrivastava K, Wu H-F. Modified silver nanoparticle as a hydrophobic affinity probe for analysis of peptides and proteins in biological samples by using liquid-liquid microextraction coupled to AP-MALDI-ion trap and MALDI-TOF mass spectrometry. *Anal. Chem* 2008;80:2583–2589. [PubMed: 18324794]
8. Lee J-S, Ulmann PA, Han MS, Mirkin CA. A DNA–gold nanoparticle-based colorimetric competition assay for the detection of cysteine. *Nano Lett* 2008;8:529–533. [PubMed: 18205426]
9. Glomm WR. Functionalized gold nanoparticles for applications in bionanotechnology. *J. Dispersion Sci. Technol* 2005;26:389–414.

10. Pitsillides CM, Joe EK, Wei X, Anderson RR, Lin CP. Selective cell targeting with light-absorbing microparticles and nanoparticles. *Biophys. J* 2003;84:4023–4032. [PubMed: 12770906]
11. Liedberg H, Lundberg T. Silver alloy coated catheters reduce catheter-associated bacteriuria. *Br. J. Urol* 1990;65:379–381. [PubMed: 2187551]
12. Gosheger G, Hardes J, Ahrens H, et al. Silver-coated megaendoprostheses in a rabbit model – an analysis of the infection rate and toxicological side effects. *Biomaterials* 2004;25:5547–5556. [PubMed: 15142737]
13. Jeong SH, Yeo SY, Yi SC. The effect of filler particle size on the antibacterial properties of compounded polymer/silver fibers. *J. Mater. Sci* 2005;40:5407–5411.
14. Yuranova T, Rincon AG, Bozzi A, et al. Antibacterial textiles prepared by RF-plasma and vacuum-UV mediated deposition of silver. *J. Photochem. Photobiol. A* 2003;161:27–34.
15. Chou W-L, Yu D-G, Yang M-C. The preparation and characterization of silver-loading cellulose acetate hollow fiber membrane for water treatment. *Polym. Adv. Technol* 2005;16:600–607.
16. Ratte HT. Bioaccumulation and toxicity of silver compounds: a review. *Environ. Toxicol. Chem* 1999;18:89–108.
17. Gupta A, Maynes M, Silver S. Effects of halides on plasmid-mediated silver resistance in *Escherichia coli*. *Appl. Environ. Microbiol* 1998;64:5042–5045. [PubMed: 9835606]
18. Matsumura Y, Yoshikata K, Kunisaki S-I, Tsuchido T. Mode of bactericidal action of silver zeolite and its comparison with that of silver nitrate. *Appl. Environ. Microbiol* 2003;69:4278–4281. [PubMed: 12839814]
19. James, GV. *Water Treatment; A Survey of Current Methods of Purifying Domestic Supplies and of Treating Industrial Effluents and Domestic Sewage*. 4th Edition. Technical Press; London, UK: 1971. p. 311
20. Baker C, Pradhan A, Pakstis L, Pochan DJ, Shah SI. Synthesis and antibacterial properties of silver nanoparticles. *J. Nanosci. Nanotechnol* 2005;5:244–249. [PubMed: 15853142]
21. Morones JR, Elechiguerra JL, Camacho A, et al. The bactericidal effect of silver nanoparticles. *Nanotechnology* 2005;16:2346–2353.
22. Dunn K, Edwards-Jones V. The role of Acticoat with nanocrystalline silver in the management of burns. *Burns* 2004;30(Suppl 1):S1–S9. [PubMed: 15327800]
23. Plyuto Y, Berquier J-M, Jacquiod C, Ricolleau C. Ag nanoparticles synthesised in template-structured mesoporous silica films on a glass substrate. *Chem. Commun. (Cambridge)* 1999;17:1653–1654.
24. Rivas L, Sanchez-Cortes S, Garcia-Ramos JV, Morcillo G. Growth of silver colloidal particles obtained by citrate reduction to increase the Raman enhancement factor. *Langmuir* 2001;17:574–577.
25. Tan Y, Jiang L, Li Y, Zhu D. One dimensional aggregates of silver nanoparticles induced by the stabilizer 2-mercaptobenzimidazole. *J. Phys. Chem. B* 2002;106:3131–3138.
26. Zhang Z, Patel RC, Kothari R, Johnson CP, Friberg SE, Aikens PA. Stable silver clusters and nanoparticles prepared in polyacrylate and inverse micellar solutions. *J. Phys. Chem. B* 2000;104:1176–1182.
27. Raveendran P, Fu J, Wallen SL. Completely green synthesis and stabilization of metal nanoparticles. *J. Am. Chem. Soc* 2003;125:13940–13941. [PubMed: 14611213]
28. Huang H, Yang X. Synthesis of polysaccharide-stabilized gold and silver nanoparticles: a green method. *Carbohydr. Res* 2004;339:2627–2631. [PubMed: 15476726]
29. Saliba MJ Jr. Heparin in the treatment of burns: a review. *Burns* 2001;27:349–358. [PubMed: 11348743]
30. Lee JY, Spicer AP. Hyaluronan: a multifunctional, megaDalton, stealth molecule. *Curr. Opin. Cell Biol* 2000;12:581–586. [PubMed: 10978893]
31. Laurent TC, Fraser JR. Hyaluronan. *FASEB J* 1992;6(7):2397–2404. [PubMed: 1563592]
32. Kemp MM, Kumar A, Mousa S, et al. Synthesis of gold and silver nanoparticles stabilized with glycosaminoglycans having distinctive biological activities. *Biomacromolecules* 2009;10:589–595. [PubMed: 19226107]
33. Nadkarni VD, Pervin A, Linhardt RJ. Directional immobilization of heparin onto beaded supports. *Anal. Biochem* 1994;222:59–67. [PubMed: 7856872]

34. Mousa SA, Linhardt R, Francis JL, Amirkhosravi A. Anti-metastatic effect of a non-anticoagulant low-molecular-weight heparin versus the standard low-molecular-weight heparin, enoxaparin. *Thromb. Haemostasis* 2006;96:816–821. [PubMed: 17139378]
35. Steinberg DA, Hurst MA, Fukii CA, et al. Protegrin-1: a broad-spectrum, rapidly microbicidal peptide with *in vivo* activity. *Antimicrob. Agents Chemother* 1997;41:1738–1742. [PubMed: 9257752]
36. Yan H, Hancock REW. Synergistic interactions between mammalian antimicrobial defense peptides. *Antimicrob. Agents Chemother* 2001;45:1558–1560. [PubMed: 11302828]

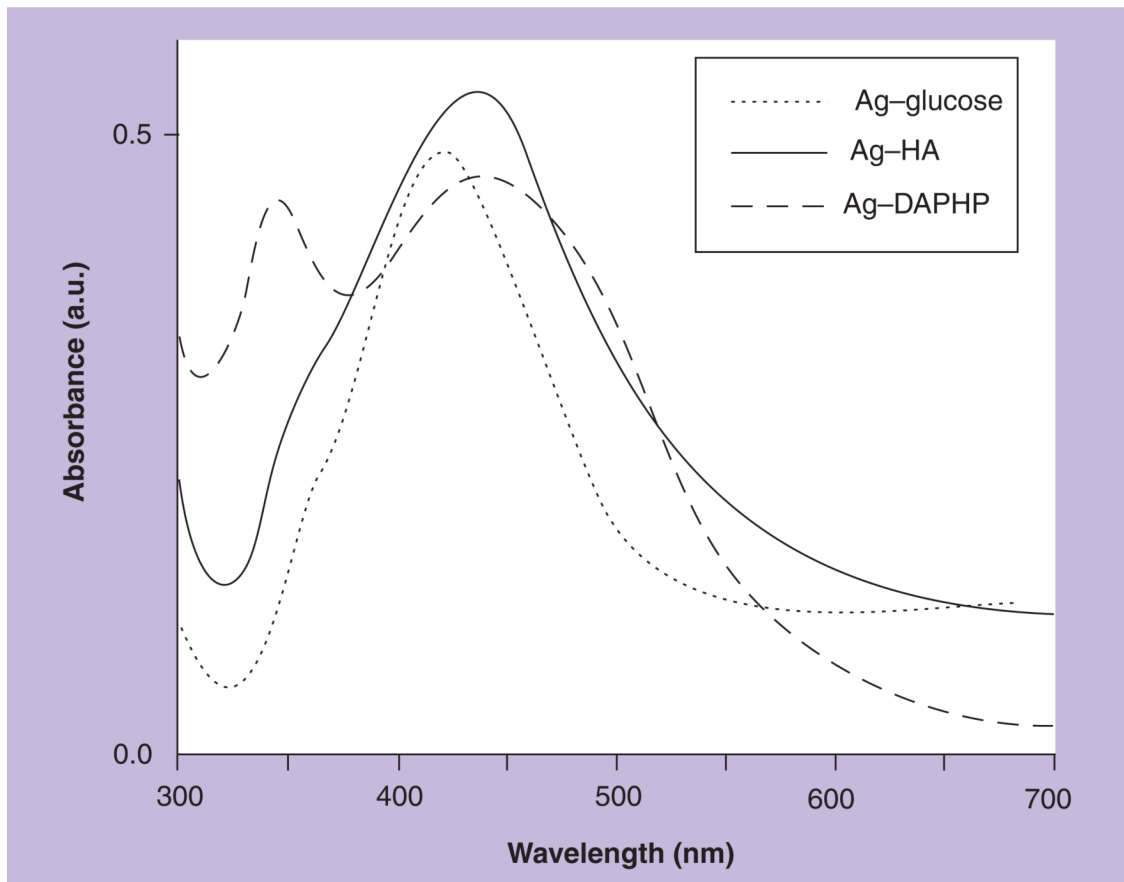


**Figure 1. UV-visible spectra of silver (Ag)-glucose, Ag-hyaluronan and Ag-diaminopyridinylated heparin nanoparticles**

The plasmon peak at approximately 400–450 nm corresponds to the formation of Ag nanoparticles. The small peak at 300 nm for the Ag-DAPHP corresponds to the absorbance from the diaminopyridine present.

Ag: Silver; a.u.: Absorbance units; DAPHP: Diaminopyridinylated heparin; HA: Hyaluronan.

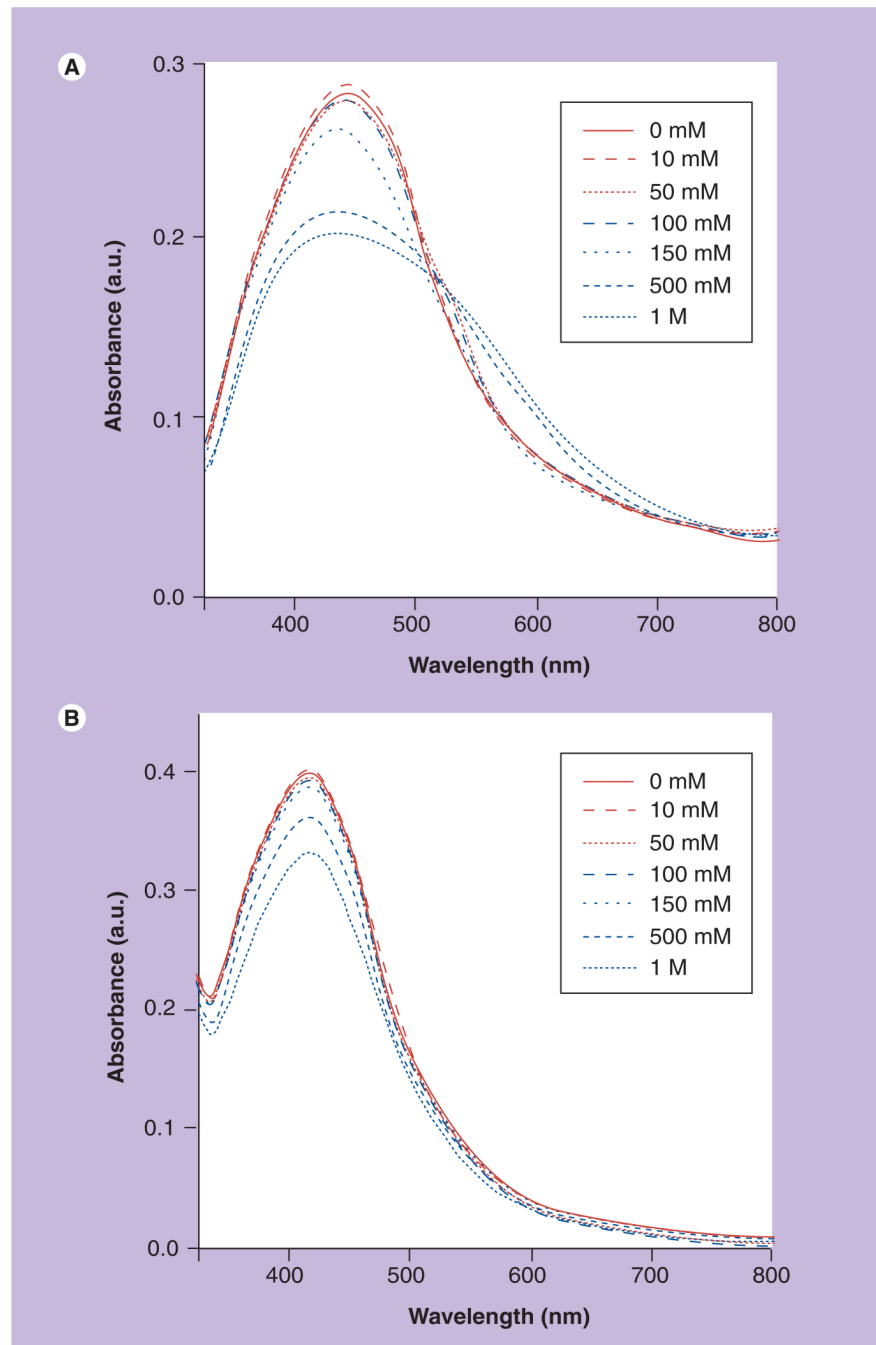


**Figure 2.** UV-visible spectra of (A) silver–diaminopyridinylated heparin as a function of increasing NaCl concentration from 0 to 1 M, and (B) silver–hyaluronan as a function of increasing NaCl concentration from 0 to 1 M  
a.u.: Absorbance units.

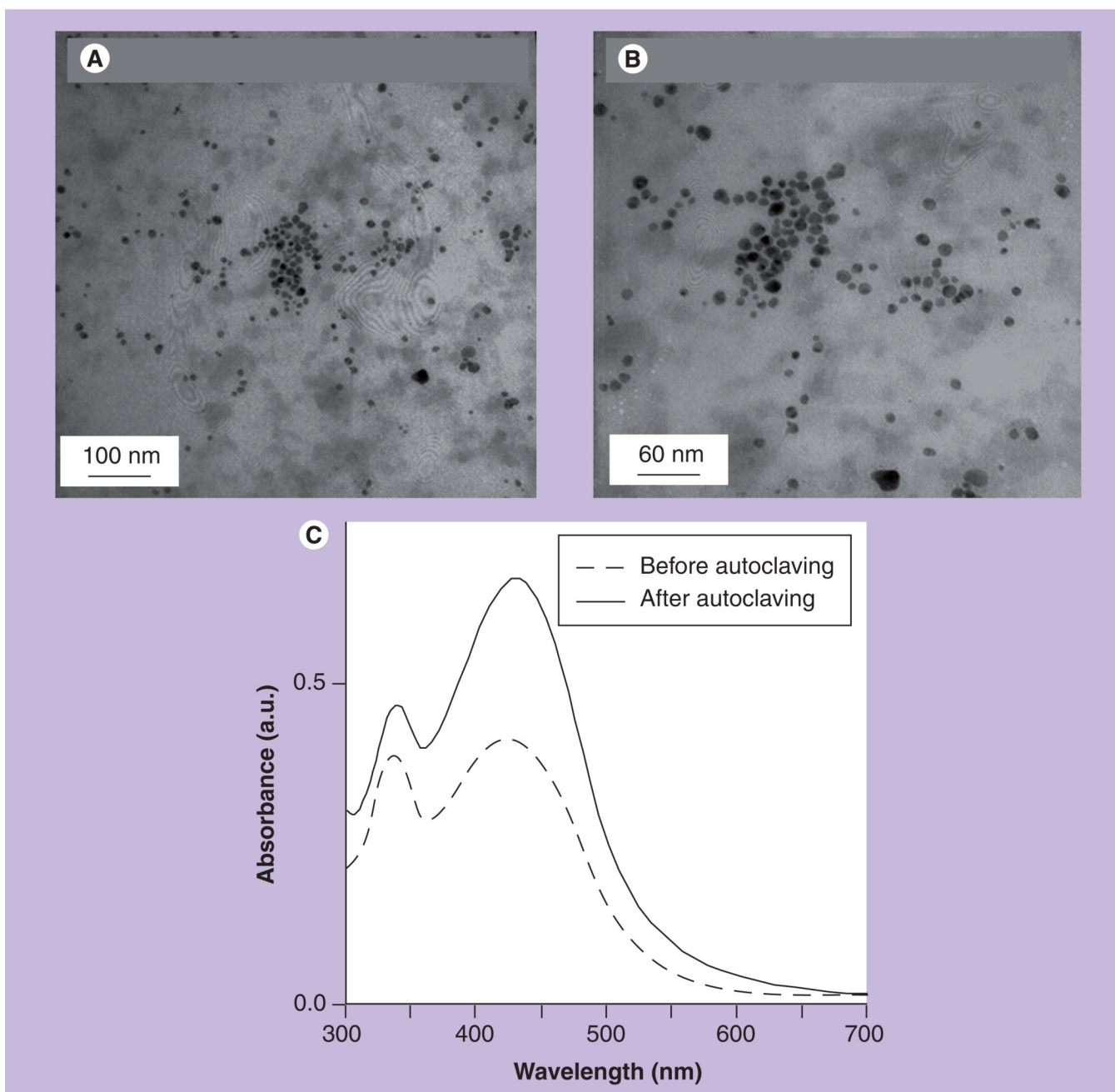


**Figure 3.** Transmission-electron microscope image of silver–diaminopyridinylated heparin at a magnification of (A)  $\times 100k$  and (B)  $\times 160k$ , and (C) UV-visible spectra before and after autoclaving a.u.: Absorbance units.

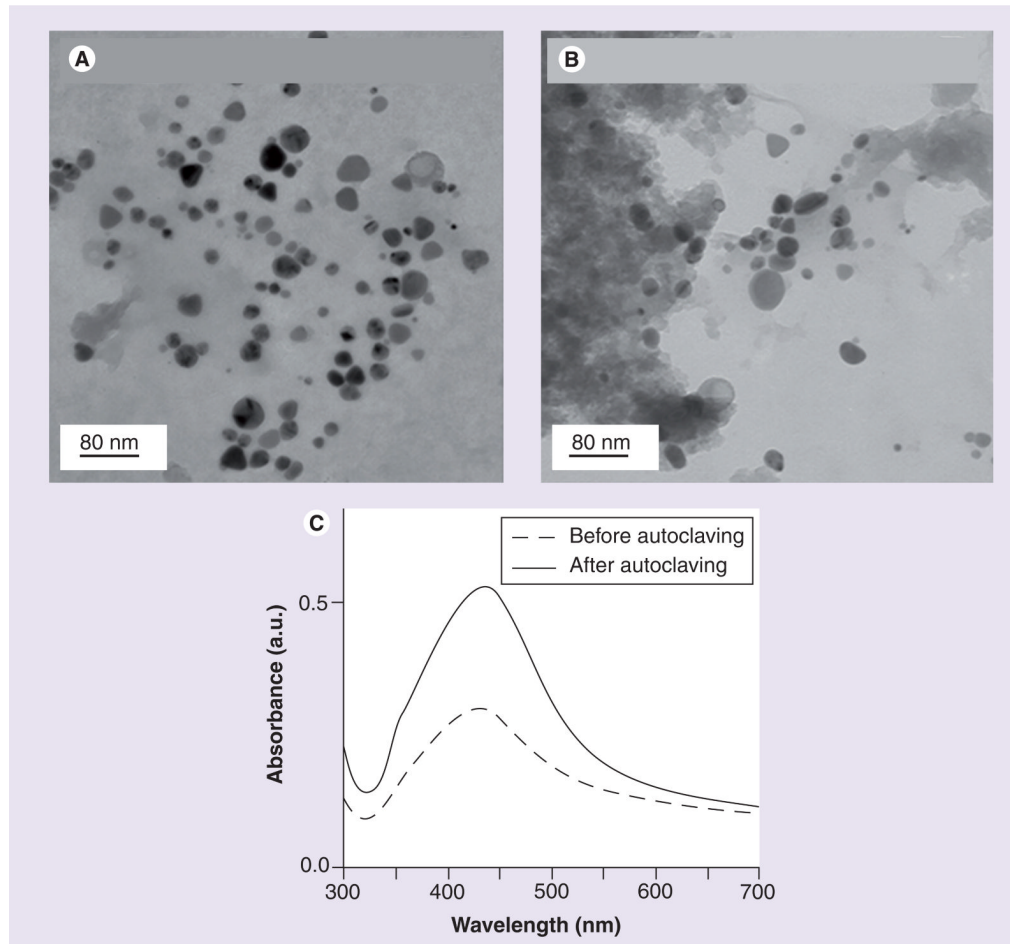


**Figure 4.** Transmission-electron microscope image of silver-hyaluronan at a magnification of (A)  $\times 125k$  and (B)  $\times 125k$ , and (C) UV-visible spectra before and after autoclaving a.u.: Absorbance units.

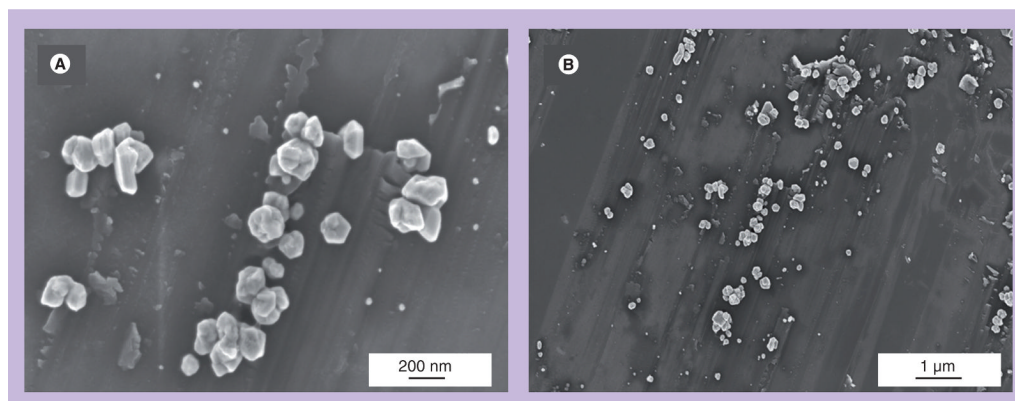


**Figure 5.** Scanning-electron microscope image of silver-hyaluronan at a magnification of (A)  $\times 93k$  and (B)  $\times 25k$ .

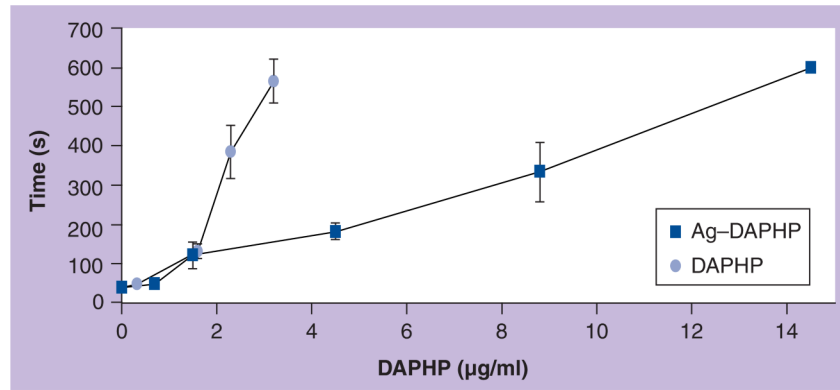


**Figure 6. The activated partial thromboplastin time assay of diaminopyridinylated heparin (dAPHP) and silver-dAPHP**

Fibrometer was manually stopped after 600 s.

Ag: Silver; DAPHP: Diaminopyridinylated heparin.

**Table 1**

Antimicrobial activity of silver nanocomposites.

Sample tested	MIC against <i>Staphylococcus aureus</i> ( $\mu\text{M}$ of sugar)	MIC against <i>Escherichia coli</i> ( $\mu\text{M}$ of sugar)
Ag-HA	$0.025 \pm 0.005$	$0.1 \pm 0.01$
Ag-DAPHP	$0.1 \pm 0.01$	$>0.1^*$
Ag-glucose	$>0.1^\ddagger$	$>0.1^\ddagger$
HA	$>1.0$	$>1.0$
DAPHP	$>1.0$	$>1.0$

Data represent mean  $\pm$  standard error of mean, n = 3.

Ag: Silver; DAPHP: Diaminopyridinylated heparin; HA: Hyaluronan; MIC: Minimum inhibitory concentration.

\* Percent inhibition ranged from 20 to 30%.

$^\ddagger$  Percent inhibition ranged from 0 to 10%.